Mesoscale Temperature Changes in the Supersonic Transport Climb Region

CARL W. KREITZBERG

Air Force Cambridge Research Laboratories, Bedford, Mass.

(Manuscript received 9 May 1967, in revised form 19 June 1967)

ABSTRACT

Supersonic transport (SST) fuel consumption is very sensitive to ambient temperatures in the region of climb from 25,000 to 52,000 ft within 200 n mi and 20 min of takeoff. It has been suggested in the literature that extensive sounding networks may be required to provide adequate temperature forecasts for SST operations.

The thermal wind relation implies that the mean temperature in this deep layer will not change rapidly in space or time and that wind shears can be used as predictors of the changes. An empirical study using the Project Stormy Spring mesoscale rawinsonde network data confirms the thermal wind implication that these mesoscale temperature changes are small. Only 6-hr soundings at a single site near the airport are required for reasonably efficient SST operation. However, predictions based on wind shear explain only about 20% of the variance of the observed temperature changes.

1. Introduction

The sensitivity of supersonic transport (SST) operation to ambient temperatures has been analyzed by Nelms (1964). The conclusions indicate that in SST design the climatology of temperature is important and that in SST operation the short-term prediction of temperature is important. In particular, SST fuel consumption is very sensitive to temperature in the transonic and supersonic acceleration region. Nelms concludes that additional frequent soundings in the vicinity of SST terminals may be required for SST operations.

Nelms estimates that two-thirds of the additional fuel necessitated by an uniformly excessive temperature in-flight would be consumed in the region between 25,000 and 52,000 ft, within 200 n mi and 20 min of takeoff. A temperature excess of 11.1C in this region would necessitate consumption of 4350 lb extra fuel or 2.3% of the total fuel consumed on a flight. This extra fuel could displace 20 passengers and baggage if gross weight is a critical factor. Nelms points out repeatedly that such figures are for a typical flight and will vary but a small amount depending on the particular flight and the aircraft design.

In a statistical study of mesoscale rawinsonde data, Nee (1966) concludes that, for his sample, precautions against the excessive temperature, which has an 18% probability of occurrence, will require 2000 lb extra fuel for ascent 20–45 n mi from a sounding and 4000 lb extra fuel for a takeoff 6 hr after a sounding.

This paper presents observational evidence and physical reasons for concluding that the variability of the mean temperature in the critical acceleration region is small and that extensive additional soundings will not be required for SST operations.

2. Thermal wind implications

The thermal wind equation relates the horizontal gradient of the mean temperature in a layer ($\nabla_p \bar{T}$) to the thermal wind, the change of the geostrophic wind in that layer $\Delta \mathbf{V}_g$. Specifically (Haltiner and Martin, 1957),

$$\frac{\Delta \mathbf{V}_g}{\Delta z} = -\left(\frac{g}{f\bar{T}}\right)\nabla_p \bar{T} \times \mathbf{k}. \tag{1}$$

For thick layers (large Δz), synoptic scale experience suggests that $\Delta \mathbf{V}_g$ can be approximated by the change in the actual wind $\Delta \mathbf{V}$. With this approximation and typical values of $\bar{T}=225$K and Coriolis parameter $f=10^{-4}$ sec^{-1} at 43° latitude, the thermal wind relation becomes

$$\nabla_p \bar{T}[^\circ\text{C}(100\text{ km})^{-1}] = 0.23\left(\frac{\Delta \mathbf{V}(\text{m sec}^{-1})}{\Delta z(\text{km})}\right) \times \mathbf{k}. \tag{2}$$

Therefore, for each 1C (100 km)$^{-1}$ change in the horizontal gradient of mean temperature of the 7–16 km (~25–52 kft) layer, the wind change would be ~39 m sec^{-1} or ~78 kt. A change of 5.1C (which corresponds to a 2000-lb change in fuel consumption) in 100 km would imply about a 200 m sec^{-1} wind change in 9 km which is more than is observed. Nevertheless, one may question the validity of applying thermal wind reasoning to mesoscale problems, and if one considers temperature predictions out to 6 hr and up to 200 n mi from the time and place of observation, a more careful examination of temperature variability is required.

Notice that the approximate form of the thermal wind relation (2) implies that the observed temperature

and the vertical wind shear can be used to estimate the temperature at other than the observation point using the first-order Taylor expansion,

$$T(S_1)=T(S_0)+\left(\frac{\partial T}{\partial S}\right)_0(S_1-S_0).$$

Furthermore, taking the dot product of the layer mean wind $\bar{\mathbf{V}}$ with Eq. (2) gives an expression for the horizontal advective temperature change $A_{\bar{T}}$, namely

$$A_{\bar{T}}(^\circ\text{C hr}^{-1})=-0.036\bar{\mathbf{V}}(\text{m sec}^{-1})\cdot\nabla_p\bar{T}[^\circ\text{C(100 km)}^{-1}]$$
$$=-0.0083\bar{\mathbf{V}}(\text{m sec}^{-1})\cdot\left(\frac{\Delta\bar{\mathbf{V}}(\text{m sec}^{-1})}{\Delta z(\text{km})}\right)\times\mathbf{k}. \quad (3)$$

Since the local temperature change $\partial\bar{T}/\partial t$ is usually proportional to $A_{\bar{T}}$, one may be able to statistically predict temperature changes with time at a site using $A_{\bar{T}}$ as a predictor.

3. Mesoscale temperature variability

Mesoscale temperature variability was analyzed by Nee (1966) by computing time and space variability of temperature at constant levels. He evaluated such variability at levels up to 60,000 ft and drew conclusions regarding the effects of such variability on SST operations. He concluded that substantial changes in fuel consumption must be allowed for in view of his rms variability statistics.

However, the variability of SST fuel consumption will not depend upon the variability of temperature at levels; rather, it will depend upon the variability of some integrated or mean temperature of the critical climbout layer. Extreme temperature changes are observed at levels, but extreme changes in the mean temperature of a deep layer have not been found in this study nor are they to be expected in view of the geostrophic wind changes they imply. It is difficult to conceive of geostrophic wind changes from 400 to 100 mb in excess of 200 m sec^{-1}, and this extreme condition corresponds to only a 5.1C (100 km)$^{-1}$ horizontal gradient of the layer mean temperature.

An example of extreme temperature change at the levels in question has been presented by Long (1966). He described an unusual 7C cooling in 99 min near a line of tall thunderstorms. The change in layer mean temperature (from 250 to 100 mb in his diagram) was only -0.7C showing an order of magnitude reduction of layer mean temperature change over the change in temperature at a level in this extreme condition. Measurements during a moderately intense cyclone (Storm 4, discussed below) have shown that the 300-mb temperature has 2.7 times the variability of the 400–200 mb mean temperature (sample size=40).

Empirical evidence showing that mesoscale variations of layer mean temperature is only one-half of the values for levels shown by Nee (1966) has been compiled from the Project Stormy Spring rawinsonde data. These data were obtained from the network shown in Fig. 1. This network operated during five stormy periods in March and April 1965 and data from three storms of different intensity have been examined.

The layer considered in one storm was 400–200 mb (~25–40 kft). This is the transonic acceleration region referred to as critical with regard to temperature by Nee (1966). On the other hand, Nelms (1964) considers the transonic plus supersonic acceleration regions (25–52 kft or ~400–100 mb) to be critical for fuel consumption. Serebreny (1965) shows fuel consumption values in his Table 1 which demonstrate that fuel consumption to 52 kft is not well specified by the 25–40 kft temperature anomaly. Therefore the 400–100 mb temperature changes were examined in two of the storms.

The rawinsonde data from Project Stormy Spring were converted to punched cards and processed by computer (Kreitzberg and Brockman, 1966). Mean temperatures for 50-mb layers were computed weighting with $p^{0.286}$. The layer mean temperatures referred to in this report are equally weighted averages of these 50-mb layer means for the 400-200 mb layer values and means computed hydrostatically from the thicknesses for 400–100 mb layer values.

Changes in layer mean temperature were computed for time changes of from 1.5 to 12 hr and for space

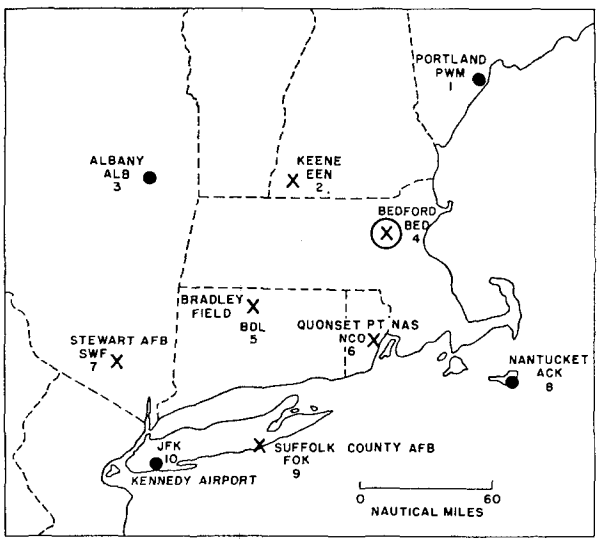

HANSCOM FIELD, BEDFORD: AFCRL RAWINSONDES AT 90 MINUTE INTERVALS INCLUDING SOME OZONESONDES.

AIR WEATHER SERVICE: MOBILE RAWINSONDES AT 90 MINUTE INTERVALS.

WEATHER BUREAU RAWINSONDES AT 3 HOUR INTERVALS.

FIG. 1. Rawinsonde network for Project Stormy Spring.

changes over distances of from 100 to 350 km. An attempt was made to measure as many space changes across the wind flow as along it. The station spacing was such that space changes could best be grouped for distances of 100, 230 and 300 km. The maximum changes (max), root-mean-square changes (rms), and sample size N are listed in Table 1 and graphs of the time changes are shown in Fig. 2. Data are shown for three storms of various types.

Storm 4 of 15–16 April 1965 was a moderately intense occlusion with a jet core of 70 m sec^{-1}. The network operated from about 12 hr prior to jet passage to 15 hr afterwards. The 400–200 mb layer was examined in this storm with regard to both variability and predictability. Storm 1 of 17–18 March 1965 was a weaker occlusion than Storm 4 but the jet core was of comparable magnitude. Observations extended from about 6 hr before to about 12 hr after the jet core. Storm 3 of 11–12 April 1965 was the most convective storm of the five Stormy Spring cases and contained the greatest variability in many respects. The jet core was about 65 m sec^{-1} and observations ran from 6 hr before to 12 hr after core passage. The four Weather Bureau sites in Fig. 1 were not activated in this case so that all data are from the six Air Force sites making 1.5-hr releases.

The sample sizes used to get the statistics in Table 1 are reasonably large for computing variability in individual storms. Notice that Storm 3 has twice the variability of Storm 1. Also, the maximum values run about 3 times the rms values except for the longer time periods. The spatial changes over 100 km compare with time changes over 1.5–3 hr. The 230-km changes appear to be as large or larger than 300-km changes which suggests temperature oscillations of wavelength ~400–500 km.

TABLE 1. Values of maximum and rms changes of layer mean temperature for samples of size N.

		Storm 4 (400–200 mb)	Storm 1 (400–100 mb)	Storm 3 (400–100 mb)
$\Delta t=1.5$ hr	rms	0.60	0.56	0.79
	max	1.79	1.26	2.22
	N	109	41	48
$\Delta t=3$ hr	rms	0.80	0.64	1.27
	max	2.46	1.50	2.71
	N	137	65	37
$\Delta t=6$ hr	rms	1.04	0.93	2.30
	max	2.88	1.92	4.07
	N	124	47	23
$\Delta t=12$ hr	rms	1.74	1.47	
	max	4.32	2.61	
	N	92	23	
$\Delta s=100$ km	rms	0.69	0.68	0.88
	max	2.42	1.26	1.99
	N	95	26	45
$\Delta s=230$ km	rms	1.13	0.68	1.46
	max	2.92	1.23	3.50
	N	39	25	18
$\Delta s=300$ km	rms	1.12	0.39	
	max	1.98	0.91	
	N	48	43	

Such oscillations are a real feature in the mid-troposphere in Case 4 in conjunction with the mesoscale structure of the cold frontal zone. The statistics don't prove this point but the detailed temperature analyses do explain this feature of the statistics.

Fig. 2 is a graph of the max and rms values for different time intervals in Table 1. The increase of variability with time is nearly linear and smooth curves are

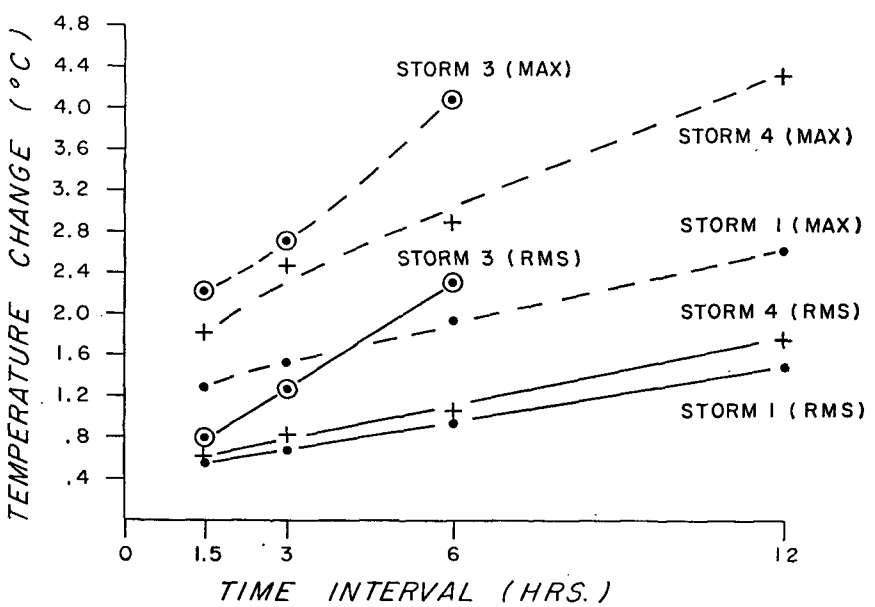

FIG. 2. Maximum (max) and rms changes in layer mean temperature as a function of time interval.

drawn in Fig. 2 approximately through the points. The rms change curves approach 0.4C at $\Delta t=0$ so this value is an estimate of the observational rms error in measuring layer mean temperature differences. This value can be compared with the 0.51C rms error found by Hodge and Harmantas (1965) in measuring temperature differences at a level.

Fig. 2 shows that variability in these mean temperatures is strongly dependent on synoptic situation. The temperature change to be exceeded only with a 5% or 1% risk for a given time interval between observations should be specified as a function of synoptic situation. For a 6-hr period the low variability cases have 5% and 1% risk temperature changes of 2C and 3C, respectively. For high variability synoptic situations the comparable figures would be 4.6 and 6.9C. Extreme values in excess of 5C (6 hr)$^{-1}$ may never occur as the thermal wind relation may limit this upper and of the spectrum in contrast to a normal frequency distribution.

Perhaps the most important point revealed by these data is that large temperature changes are not found over the shorter time and space intervals. Thus, synoptic-scale upper air data can be used for the most part to establish variability as a function of synoptic situation.

4. Mesoscale temperature prediction

The approximate thermal wind relations, Eqs. (2) and (3), suggest the magnitude of temperature changes one may expect based on knowledge of wind changes through a deep layer. One may also expect these relations to have predictive value. That is, given a sounding one can compute mean temperature and wind shear and use $\nabla_p\bar{T}$ and $A_{\bar{T}}$ from the equations as predictors of $\bar{T}$ at some point nearby in either space or time.

Such predictions were attempted using the 400–200 mb layer data in Storm 4. An example of observed and predicted space changes of $\bar{T}$ is shown in Fig. 3. The observed temperatures are plotted at the sites and isoplethed. The dashed lines extend from the sites for 100 km in the direction of $\nabla_p\bar{T}$ calculated from Eq. (2). The temperatures expected at the endpoints of the dashed lines from the magnitude of $\nabla_p\bar{T}$ are enclosed in brackets. One can see from Fig. 3 that the $\nabla_p\bar{T}$ values implied from the wind shear through Eq. (2) are not particularly accurate either in direction or magnitude. Thus, the thermal wind relation is of limited value in inferring temperature gradients even when a deep (15 kft) layer is considered.

The extent of the predictive implications of Eqs. (2) and (3) is revealed by the linear regression analysis summarized in Table 2. The regression equation is of the form

$$Y=a+(b\pm t_{0.05}s_b)X.$$

The term $t_{0.05}s_b$ is a measure of the 95% confidence level of the regression coefficient; it is the product of the sample standard deviation of b and the student "t" value at the 5% level for the appropriate degrees of freedom. For example, at $\Delta t=12$ the uncertainty in b

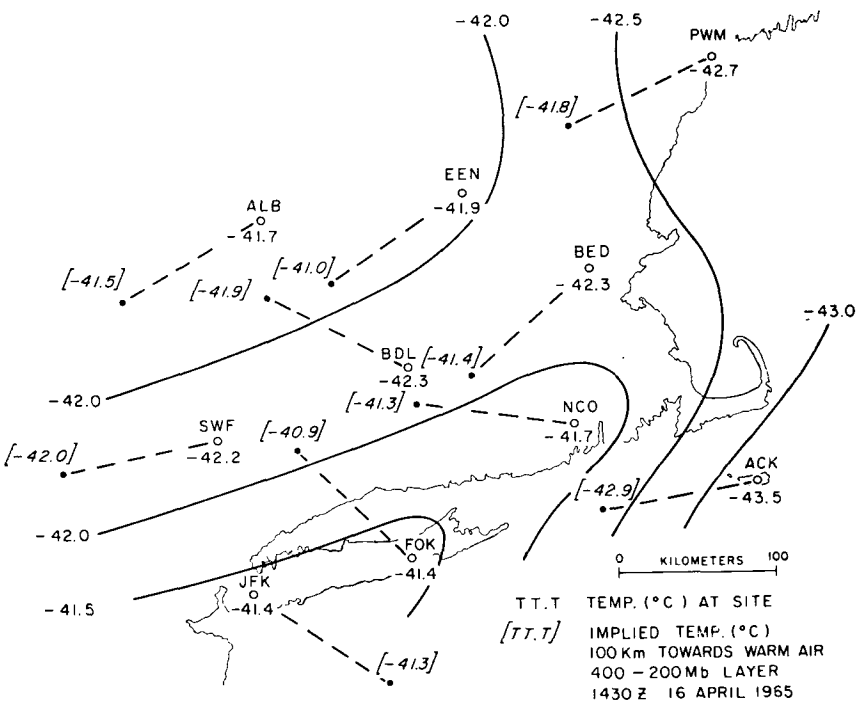

FIG. 3. Example of observed and implied temperature gradients.

TABLE 2. Regression statistics between observed and implied temperature time changes and horizontal gradients.

	$Y=\partial T/\partial t$ [°C hr^{-1}]; $X=A_{\bar{T}}$ (°C hr^{-1}) Δt (hr)						$Y=\partial T/\partial s$ [°C(100 km)$^{-1}$]; $X=\mathbf{s}\cdot\nabla_p T$ [°C (100 km)$^{-1}$] Δs (km)	
	1.5	3	4.5	6	9	12	100	200–300
N	109	137	97	124	105	92	95	87
r	0.33	0.39	0.44	0.49	0.36	0.16	0.42	0.50
a	−0.03	−0.03	−0.05	−0.04	0.00	0.06	−0.10	−0.02
b	0.20	0.16	0.15	0.15	0.10	0.03	0.45	0.36
$t_{0.05}s_b$	0.11	0.07	0.06	0.05	0.05	0.04	0.20	0.13
s_y	0.390	0.258	0.220	0.178	0.151	0.118	0.691	0.425
$s_{y\cdot x}$	0.370	0.138	0.199	0.155	0.141	0.117	0.629	0.370
IMP(%)	5	8	10	13	7	0	9	13
$s_{\Delta\bar{T}\cdot x}$	0.56	0.71	0.90	0.93	1.27	1.40	0.63	0.74–1.11

exceeds its magnitude so the correlation is not significant at the 95% level.

The correlation coefficient r reaches a maximum at $\Delta t=6$ hr meaning that the shorter term changes are either masked by noise or that the shear through the deep layer is more representative of scales on the order of 6 hr. Similarly, the shorter scale space changes are less well related to the deep layer shears than are the 200–300 km changes. Notice that the regression slopes b decrease with increasing prediction interval. Slopes for time prediction are less than for space prediction reflecting the compensating effect of vertical motion which makes $\partial\bar{T}/\partial t$ systematically less than $-\mathbf{V}\cdot\nabla_p\bar{T}$.

The sample standard deviations s_y and standard error of estimate from regression $s_{y\cdot x}$ give an idea of variability with and without the prediction equation. The improvement in percent (IMP%) is $100(s_y-s_{y\cdot x})/s_y$. The reduction in variance is about twice this measure of reduction in standard deviation. Thus, the prediction technique produces about a 10% reduction in standard deviation and a 20% reduction in variance. Notice that the best improvement is for time changes and distances of most use in SST operations, assuming that the sounding interval is 6 hr and SST ascents are made about 200 km from the sounding site.

The standard deviation of the prediction of change as a function of forecast interval is $s_{y\cdot x}$ times Δt or Δs and is listed in Table 2 as $s_{\Delta\bar{T}\cdot x}$. If these prediction errors are normally distributed then 6-hr prediction errors will exceed 2.8C only 1% of the time. Assuming independence of time and space prediction errors, the 1% error level in 6 hr and 200–200 km predictions would be 4.3C. This error corresponds to 1700 lb of fuel which should not be an unduly large reserve compared with that needed for contingencies such as alternate terminals, holding pattern or missed approach.

The somewhat poor correlation of implied and observed temperature changes shown in Table 2 may have been due only to small signal-to-noise ratios in measuring temperature change. One may be better able to predict the large temperature changes which substantially exceed the noise level. To examine this hypothesis, the joint frequencies in Table 3 were prepared for changes between stations separated by 200–300 km.

Fig. 2 has indicated that an upper limit to the rms error in measuring layer mean temperature differences is 0.4C. Since the observed gradients included in Table 3 were for sites 200 km or more apart, the gradients have an rms error of less than 0.2C(100 km)$^{-1}$. The wind change from 400–200 mb can be observed with an rms error of about 4 m sec^{-1} so that the temperature gradients computed from Eq. (2) also have an rms error due to shear error of about 0.2C(100 km)$^{-1}$.

Thus, 73 of the 87 values included in Table 3 have a magnitude larger than the rms errors in observed and/or implied temperature gradient. Nevertheless, the implied temperature gradients in Table 3 do not do a very good job of predicting even the larger values of observed temperature gradient.

5. Concluding remarks

The mean temperature in the 400–100 mb layer must be predicted to within a 3σ error of 5C if an SST is to carry but 2000 lb extra fuel with 99% confidence of not over-consuming fuel during transonic and supersonic acceleration. The observed mesoscale variability of such temperatures in three storms is so low that 6-hr observations near the terminal permit persistence forecasts to nearly meet this criteria. Furthermore, variability changes with the synoptic situation so that a "safe" fuel reserve can probably be specified as a function of the synoptic situation. Where large temperature changes may be expected, turbulence from convection or the jet stream will probably be the more critical problem.

In the three spring storms examined, the maximum observed temperature change within 6 hr and 300 km was 4.1C and 3.5C, respectively. Thus, direct observations do not indicate that temperature changes of great importance to SST operation exist on the mesoscale. The thermal wind relation shows that the geostrophic wind change from 400 to 100 mb corresponding to a layer mean temperature gradient of 5C(300 km)$^{-1}$ is 67 m sec^{-1}, or 200 m sec^{-1} for $\nabla_p\bar{T}=5\text{C}(100\text{ km})^{-1}$.

The use of vertical wind shear as a predictor of mesoscale temperature gradients is of limited value even when a 15 kft deep layer is used. The reason for this weakness of relations (2) and (3) is due not to inaccu-

TABLE 3. Joint frequency distribution of observed temperature gradients on the scale of 200–300 km and temperature gradients implied by the wind shear for the 400–200 mb layer.

Temperature gradient observed [°C (100 km)$^{-1}$]	Temperature gradient implied by the wind shear [°C (100 km)$^{-1}$]															Total
	−1.4	−1.2	−1.0	−0.8	−0.6	−0.4	−0.2	0	0.2	0.4	0.6	0.8	1.0	1.2	1.4	
1.4																
1.2								1				1				2
1.0																0
0.8												2			1	3
0.6							1	2	2	1	3					9
0.4						1		1	1	3	1	1	2	4		14
0.2			1				1	1	4	4	3	1	2		1	18
0			1			2	3		1	2	2	1				12
−0.2				1	2	2		3	1	1	1					11
−0.4			2		2		3	2		1						10
−0.6				1	1	1		1		2						6
−0.8																0
−1.0				1			1									2
−1.2																
−1.4																
Total			4	3	5	6	9	11	9	14	10	6	4	4	2	87

racy of observation but rather to the ageostrophic component of the wind shear. The limited predictive value of the approximate relations (2) and (3) does not nullify the implications of the exact equation (1).

Departing SST aircraft can record the mean temperature and these aircraft soundings can be used to update temperature predictions. This technique would work only if real time read out of the mean temperature (or fuel consumption directly) were provided for. Also, this technique will be most useful only when subsequent departures are within 6 hr or less.

This study of mesoscale variations and the implications of the thermal wind relation indicates that temperature changes of significance to the SST problem will be associated with large-scale intense jet streams which have substantial geostrophic wind shears. Therefore, the most useful tool for routine prediction of mean temperatures for SST ascents is probably the 400–100 mb synoptic-scale thickness chart. This indicator of the larger scale thermal pattern (through the hydrostatic relation of thickness to mean temperature) will show when and where substantial temperature changes are likely.

Further studies on this problem can be made for large areas and many synoptic situations simply by reference to synoptic scale 400–100 mb thickness data. An excellent case would be the 19–22 February 1964 period for which NASA (Smith, 1967) has obtained 3-hr rawinsondes throughout the southeastern United States. The synoptic situation includes an extremely intense jet stream so that temperature gradients would be relatively large.

REFERENCES

Haltiner, G. J., and F. L. Martin, 1957: *Dynamical and Physical Meteorology*. New York, McGraw-Hill Co., Inc., p. 204.

Hodge, M. W., and C. Harmantas, 1965: Compatability of United States rawinsondes. *Mon. Wea. Rev.*, **93**, 253–266.

Kreitzberg, C. W., and W. E. Brockman, 1966: Computer processing of mesoscale rawinsonde data from Project Stormy Spring. AFCRL-66-97 Spec. Rept., No. 41, 35 pp.

Long, M. J., 1966: A case of rapid cooling near the tropopause, near a line of tall thunderstorms. *J. Appl. Meteor.*, **5**, 851–856.

Nee, Paul F., 1966: Mesoscale temperature variability below 60,000 feet. *J. Appl. Meteor.*, **5**, 847–805.

Nelms, W. P., Jr., 1964: Some effects of atmospheric temperature variations on performance of the supersonic transport. NASA Rept. TMX-51563, 32 pp.

Serebreny, S. M., 1965: The interrelation of cruise fuel consumption, temperature and track selection in supersonic transport operation. *J. Inst. Navigation (London)*, **18**, 123–140.

Smith, O. E., 1967: Recent advances in dynamical and statistical meteorology to aerospace vehicle problems. NASA Rept. TMX-53649, 400 pp.